RSC Advances

PAPER

View Article Online
View Journal | View Issue

Cite this: *RSC Adv.*, 2017, **7**, 19940

Light activated non-reciprocal motion in liquid crystalline networks by designed microactuator architecture†‡

D. Martella, §[ab] D. Antonioli, §[c] S. Nocentini, [a] D. S. Wiersma, [a] G. Galli, [d] M. Laus [c] and C. Parmeggiani *[ae]

Light responsive liquid crystalline networks were prepared by photopolymerization of azobenzene-doped mesogen mixtures and applied for production of micro-actuators by a laser writing technique. Adjusting the cross-linker content was found to be an efficient and easy way to control the dynamics of light-induced deformation from the micro- up to the macro-meter length scales. Starting from a complete characterization of the response of millimeter-sized stripes under irradiation with different sources (LED and laser light), micro-structures based on different monomer mixtures were analyzed for micro-actuator preparation. Double stripes, able to perform a light driven asymmetric movement due to the different mixture properties, were created by a double step process through a laser writing system. These results are a simple demonstration of an optically activated non-reciprocal movement in the microscale by a chemical material manipulation. Moreover, we demonstrate a rapid actuator dynamics that allows a movement in the second time scale for macrostructures and a millisecond actuation in the microscale.

Received 19th March 2017
Accepted 27th March 2017

DOI: 10.1039/c7ra03224b

rsc.li/rsc-advances

Introduction

The ability to control a material's shape by different external stimuli is extensively studied for both actuating and sensing[1] devices and interest is also growing for photonic applications.[2] In the past decade, thanks to the increased possibilities offered by micro- and nano-technologies, great efforts were concentrated on the realization of tiny robotic structures from the scale of insects down to that of micro-organisms. Light figures out as one of the more appealing energy source for micro and nano-robot actuation, enabling the remote spatial and temporal control on the material responses up to the nano-scale, where other stimuli are more difficult to be implemented and batteries are not an option.

Liquid crystalline networks (LCNs) featuring a macroscopic alignment are able to deform once they undergo a liquid crystalline to isotropic phase transition. Then, the cross-linked structure allows the initial shape to be recovered after removal of the external stimulus. The type of shape-change is determined by the alignment characteristics inside the network.[3] In turn, the ordering technology can be fully exploited in the LCNs engineering to generate networks with even complex macroscopic alignment combinations. The introduction of light-sensitive molecular switches, such as azobenzene dyes[4] leads to light-activated LCNs. Robotic devices realized by means of these materials were recently prepared and studied both on macroscopic (*e.g.* motor[5] or robotic arm[6]) and microscopic scales (*e.g.* artificial cilia,[7] microwalker[8] or microswimmer[9]).

Starting from the first examples of liquid crystalline elastomers (LCE), prepared by Finkelmann by grafting mesogenic cores on a polysiloxane chain,[10] several synthetic strategies have been developed. Among them, the photo polymerization of mesogens bearing acrylate groups[11] enables the integration of complex alignments inside the polymeric matrix,[12] opening to sophisticated material deformations rather than simple contractions and expansions. Moreover, this polymerization technology is widely use in several photolithographic processes, allowing the microscale patterning of LCN by the use of masks,[13] molds[14] or more advanced techniques such as Direct Laser Writing (DLW).[15]

[a]*European Laboratory for Non-Linear Spectroscopy (LENS), Università degli Studi di Firenze, via Nello Carrara 1, 50019 Sesto Fiorentino, Italy. E-mail: camilla.parmeggiani@lens.unifi.it*

[b]*Dipartimento di Chimica "Ugo Schiff", Università degli Studi di Firenze, via della Lastruccia 3-13, 50019 Sesto Fiorentino, Italy*

[c]*Dipartimento di Scienze e Innovazione Tecnologica (DISIT), Universitá del Piemonte Orientale "A. Avogadro", Viale T. Michel 11, 15121 Alessandria, Italy*

[d]*Dipartimento di Chimica e Chimica Industriale and UdR Pisa INSTM, Università di Pisa, via Moruzzi 13, 56124 Pisa, Italy*

[e]*Consiglio Nazionale delle Ricerche – Istituto Nazionale di Ottica, Sede Secondaria di Sesto Fiorentino, via Nello Carrara 1, 50019 Sesto Fiorentino, Italy*

† Dedicated to Prof. Andrea Goti on the occasion of his 60th birthday.

‡ Electronic supplementary information (ESI) available: Mesomorphic characterization of the mixtures: DSC traces for all mixtures, ATR spectra and POM images of significant mixtures and films; bending and relaxation times and related average angular speed measured for macroscopic stripes under different excitation powers. See DOI: 10.1039/c7ra03224b

§ These authors contributed equally.

Some of us demonstrated how this latter technique, based on a two-photon polymerization, leads to 3D structures with nano-scale feature size, and also how manipulating their alignment[16] opens to the fabrication of more complex micro-robots. A notable example is the preparation of structures smaller than any walking living organisms and able to walk on different surfaces by irradiation with light.[8] Movement in the microscale is affected by forces sometimes negligible in the macroscopic world. A good example is the problem of swimming on a micrometer scale: as discussed by Purcell in his famous lecture on "life at low Reynolds number",[17] the motion of micro-organisms in a Newtonian fluid requires a sequence of movements that can not be time-reversed to lead a net motion. For this reason, preparation of LCN micro-structures able to perform asymmetric and non reciprocal motions results of extreme interest to enlarge the class of micro-robots in different environments.

In this work, we focused our attention on the modulation of the mechanical response of LCNs to perform such type of complex movements. In particular, we studied several LCNs prepared by photo polymerization of mesogenic acrylates and diacrylates in different ratios. To elucidate the role of the macromolecular architectures on the mechanical and light responsive behaviour, a dynamic-mechanical analysis under different light stimulation conditions was carried out on millimetre length scale LCNs cantilevers. The same materials were also tested at the micro-scale, thanks to the laser writing micro-fabrication, and the micro-structures behaviour was analysed under high power light stimulation. The complex relations between the mechanical and temporal response at these two different scales and the LCNs architecture was then employed to guide the design of a novel composite micro-actuator assembled by a two-step process able to integrate two different macromolecular architectures. When illuminated such micro-actuator was able to perform non-reciprocal movement.

Preparation and thermal-mechanical behaviour of macroscopic LCN films

Mixtures of the molecules depicted in Fig. 1 were employed to obtain the materials tailored for this study. **1** and **2** are mesogenic monomers and **2**, bearing two acrylate groups, acts also as a cross-linker. In fact, network formation is mandatory to obtain a reversible shape-change in the material. Adjusting the ratio between these mesogens was recently exploited to improve the resolution in DLW fabrication, showing how microstructures prepared with a high percentage of cross-linker are suitable for creation of suspended straight elements with very good resolution.[18] The azobenzene containing monomer **3** was also added to obtain a photo-responsive material and the initiator, Irgacure 369, was employed to trigger the photo polymerization.

Different monomeric mixtures, listed as **MM*x***, where *x* is the percentage of the cross-linker **2**, differing only in the cross-linker percentage were prepared according to previous studies (See Table S1 in ESI†).[15] The complete mesomorphic characterization of the mixtures investigated by Differential Scanning Calorimetry (DSC) and Polarized Optical Microscopy (POM), is reported in ESI (Table S1 and Fig. S1†). The mixtures, after infiltration in appropriate cells, were aligned in the nematic phase and then irradiated with an UV LED lamp thus leading to the macroscopic polymeric films. Optimal polymerization conditions were determined by monitoring the process with time using FT-IR spectroscopy, as illustrated in Fig. S2.† After polymerization, the films were removed from the cells and analyzed for their thermal and mechanical behavior.

The thermo-mechanical characteristics of the films were determined by DMTA. The samples were tested in tensile mode as a function of temperature and at constant temperature (room temperature) once subjected to cyclic irradiation conditions. The storage modulus (E′) and the loss factor (tan δ) were determined as a function of temperature only for films analyzed in the parallel direction with respect to the liquid crystalline alignment. Premature break of the film occurred across the glass transition when the samples were analyzed in the perpendicular direction. Fig. 2a and b report the trend of E′ and tan δ, respectively, as a function of temperature. At low temperatures, the E′ values were on the same order of magnitude (1.0–2.0 GPa at −25 °C) and increased regularly as the cross-linking degree rose. The modulus decreased by two orders of magnitude in the range 0–60 °C due to the glass transition. The plateau modulus at temperatures above the glass transition scaled linearly with the cross-linking degree, as is typically

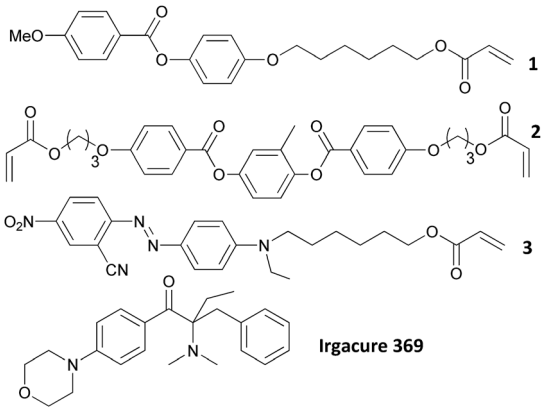

Fig. 1 Structures of chemicals used for LCN preparation.

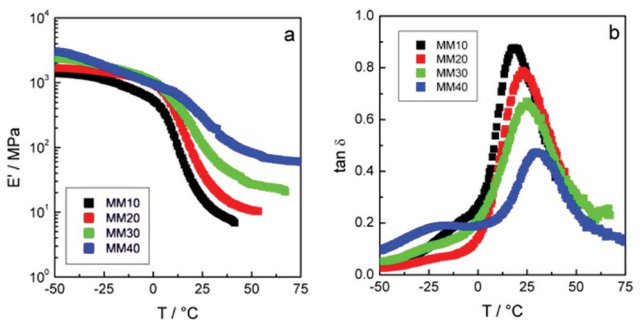

Fig. 2 Trends of E′ (a) and tan δ (b) for the films prepared by mixtures **MM10**–**MM40** analyzed along the direction parallel to the liquid crystalline alignment.

observed in cross-linked samples. From −25 °C to 60 °C, tan δ appeared structured in two components thus suggesting also the occurrence of a secondary relaxation process, partially superposed to the glass transition, attributed to the relaxation modes of the mesogenic units. The glass transition temperature increased with the cross-linking degree whereas the maximum of the tan δ regularly decreased, thus indicating that the lossy behavior of the material was progressively reduced. Nevertheless, the observed tan δ values were higher than those previously reported for cross-linked polymers from mesogenic diacrylates or similar mixtures.[19] DSC analysis confirms the glass transition temperature values (Fig. S3†). Although endothermic peaks (around 110–120 °C) were present in the DSC traces of **MM10** and **MM20**, POM observations (Fig. S4†) revealed a significant degree of birefringence in all the polymeric films up to at least 150 °C. This behavior is possibly due to residual stress birefringence, analogous to other LCNs with similar structure where T_{NI}, not clearly detectable, was located around 200 °C.[11,13,19,20]

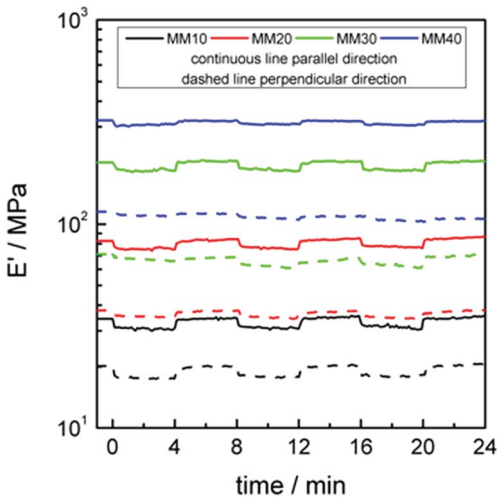

Fig. 3 Trend of E′ for the films prepared from mixtures **MM10–MM40** analyzed at room temperature along the direction parallel and perpendicular to the liquid crystalline alignment once subjected to the cyclic light stimulation (a static + dynamic load of 15 g is applied).

Light actuation for LCN macroscopic films

Irradiation with selective wavelengths is able to induce the *trans–cis* isomerization in azobenzenes[21] contained in the LCNs. In turn, this local azobenzene deformation can be propagated along the LC structure and induce disordering effects extending over large distances. From a mechanical point of view, this effect could result in a change of the polymeric chain configuration thus resulting in light-driven macroscopic deformations. The azobenzene used in this study is a push–pull system very similar to the one previously reported,[22] in which the percentage of the *cis* isomer at the photostationary state is less than 10% and the thermal *cis* to *trans* isomerization kinetics is very fast (in the order of microseconds). To elucidate the light-induced mechanical effects in the present polymeric networks, a DMTA analysis was performed at room temperature, in the parallel and the perpendicular direction of the films with respect to the liquid crystalline alignment, under the cyclic light stimulation of a green LED lamp. In more detail, the films were fixed in the DMTA tensile geometry, in both the perpendicular and parallel directions, and subjected to a static load and to a superposed dynamic load at 1 Hz frequency. After ten minute equilibration time, the green lamp was switched on and off for four minutes. This cycle was repeated three times and the modulus variation, as well as the film deformation, were recorded as function of time (Fig. 3). The temperature was constantly monitored during the cycles and only minor changes (<1 °C) were observed thus indicating that the mechanical response to the light stimulation occurs at constant temperature. In all cases, E′ decreased when the lamp was switched on and recovered its initial value when the lamp was switched off. These modulus changes occurred in 10–20 seconds. No fatigue effects appeared, at least for investigated irradiation cycles. The modulus and the modulus drop due to the light irradiation were both higher along the parallel direction than in the perpendicular one.

The same procedure was applied by changing the total (static + dynamic) load (Fig. 4a and b) and then the effect of the light irradiation on the film deformation was determined by extrapolating the mechanical data to zero load, as sketched in Fig. 4c.

On plotting the deformation data at zero stress against the cross-linking degree, a dual behavior appeared in which the films subjected to light irradiation displayed a contraction in the parallel direction and an expansion in the perpendicular direction. The effect of cross-linking degree is not obvious in azobenzene containing LCNs: while in some cases a decrease in the light-induced deformation is observed by increasing the cross-linker percentage,[23] an opposite behavior is reported in other examples.[24] In our polymers the deformation extent increased regularly as the cross-linking degree increased.

The ratio between the deformation perpendicular and parallel to the director decreased from −0.12 to −0.36 as the cross-linking degree increased, thus indicating that a volume loss occurred during the green light illumination, in qualitative agreement with literature data.[25] The overall picture of the mechanical data indicates an increased effectiveness of the azobenzene units to propagate the local distortion due to the light-induced *trans–cis* isomerization to the LCN structure as the cross-linking degree increases. This stems from a progressive increase in the coupling efficiency between the dynamics of the light responsive azobenzene and the network structure *via* the liquid crystalline field when the network mesh size decreases due to the increase in the crosslinking degree. This effect results especially effective at the very low loadings (1% mol) of azobenzene units. However, due to such small amount of azobenzene, the overall mechanical response to the light stimulation by the adopted lamp is rather small (around 1% of the initial length). This indicates that the local disordering of the azobenzene moieties produces a limited evolution of the

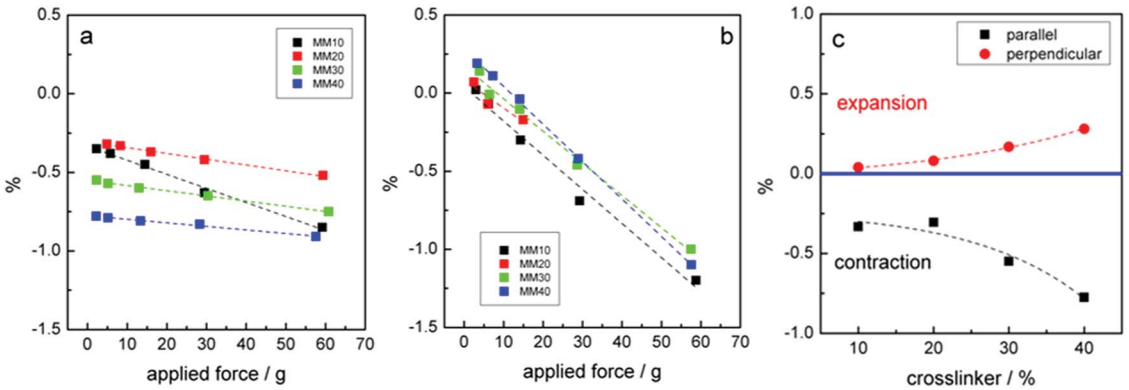

Fig. 4 Effect of light irradiation on the deformation once the film were subjected to different total (static + dynamic) loads. Deformation as a function of the cross-linking degree in uniaxial planar films measured parallel (a) and perpendicular (b) to the director. Deformations % in length extrapolated at zero stress (c).

network chains from the anisotropic configuration to the random coil configuration, which represents the most favorable entropic state. Larger deformations were observed in LCNs containing much higher overall amounts of azobenzene units that were incorporated into the network structure as both side chains and cross-linkers.[23] Due to the nature of our system, we exploited the photothermal effect where the dyes act mainly as nanoscale heaters. The temperature rise is able, in fact, to effectively push the network chains toward the most favourable configuration. This mechanism is appealing for robotics and photonics due to the LCN characteristic response time, in the millisecond scale,[8] which enables a true real time device control by tuning the irradiation power.[26]

In this case, the most suitable alignment state for the LCNs is the splayed geometry[27] because, in our setup, the non-Gaussian laser focal spot and the not exactly reproducible tip mechanical constraints make measurement on uniaxial aligned films more difficult and less accurate.

Light-induced deformations of splayed LCN films were then studied by irradiation from the top with a green laser. Light passed through the whole thickness of the film independently from the cross-linker percentage in the different mixtures. The penetration length was evaluated to be 6 μm by transmission measurement of a green laser light across the film. Such films display controlled bending as function of temperature. Fig. 5a shows the relationship between the laser power and the induced bending angle and Fig. 5c reports the photos obtained for the splayed **MM30** sample during irradiation. Even though the bending power threshold was found rather similar in all samples (around 0.41 mW mm^{-2}), the bending angles resulted very different, with bigger angles for less cross-linked films, especially at low irradiation powers (*e.g.* 160° for **MM10** and 20° **MM40** by irradiation with 0.84 mW mm^{-2}). By increasing the laser power, the bending angle increased gradually at first and then more steeply until the complete folding of the cantilevers on themselves. The response times (both for bending and recovery) for all mixtures are reported in Table S1,† while representative data are shown in Fig. 5b. On increasing the laser power, the response time became faster due to the higher number of absorbed photons that caused a higher local temperature. In case of the highest power levels (0.84 and 1.2 mW mm^{-2}), bending time of less than 1.5 s and recovery time of about 1.3 s are observed for all the mixtures except for **MM10**, that moved slower (see Table S2†). Bending deformation rate and recovery times decreased by increasing the cross-linking degree for each laser power level employed, probably due to the corresponding modulus increase in the samples.

Although a complete analysis for the recovery times is difficult, they were independent on the bending angle (and therefore of the laser power) because the relaxation dynamics is due only to the thermal conductivity of the material, while the actuation time is strictly connected to the power density absorbed by the film.

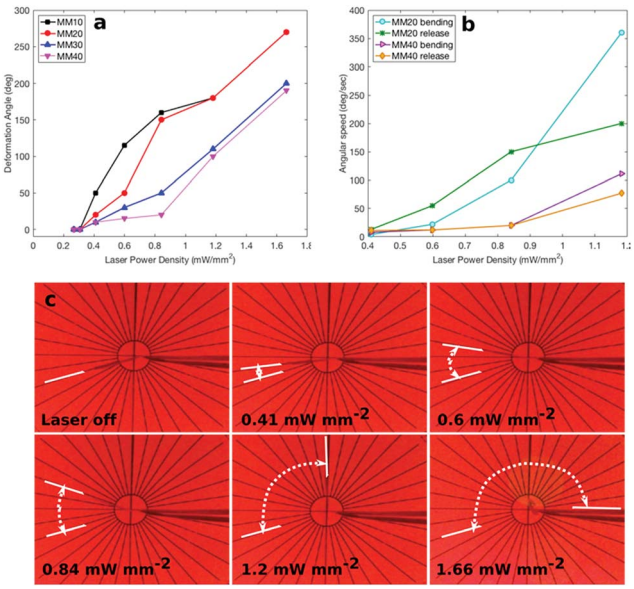

Fig. 5 Response of splayed films to laser irradiation. (a) Bending angle as a function of laser power for all mixtures; (b) angular speeds for MM20 and MM40; (c) photos showing splayed MM30 film response during irradiation at increasing laser power density.

A deeper comparison of the mixture response times is not possible, because of the non-Gaussian laser focal spot and the not exactly reproducibility of the mechanical constraints at the tip. The analysis of data on both homogenous films (by DMA) and splayed ones (by laser irradiation) showed how the molecular parameters play different roles in the pure optic stimulation and in the combined photo and thermal stimulation. Whereas at constant temperature the light-induced mechanical effects are limited, the driving force exerted by the combination of photo and thermal laser stimulations appears much more effective to promote the network deformation. In this case, the high elastic modulus due to the increased cross-linking densities determines a slower mechanical response, also in the recovery dynamics.

Light-induced shape-change in LCN micro-structures

LCN micro-structures were prepared by DLW according to a methodology previously described.[18] By this technique, we achieved the polymerization of a single voxel of polymer by focusing the laser beam inside monomer mixture after the alignment process. Only in the focal spot, the high intensity of power allows the two-photon absorption by the photo-initiator inducing polymerization in the focal spot. Different 3D structures can be prepared by scanning the focal position of the laser with respect to the polymerization cell.

First, we fabricated blocks ($100 \times 20 \times 10$ μm^3) with homogeneous alignment, as verified by the angular dependence of transmittance extinction in POM observation (Fig. 6a and b).

The homogeneous alignment was selected to have a complete comparison of mixture performances: in such scale, an exhaustive analysis results easier for contraction movements (Fig. 6c and d) than for bending. Table 1 shows the maximum contraction percentage and the response time for each block. Maximal contraction was higher (19%) and actuation speed was faster (*e.g.* v_{cont} 1.26 $\mu m\ ms^{-1}$) for the least densely cross-linked **MM10**, while they were lower (10%) and slower (*e.g.* v_{cont} 0.5 $\mu m\ ms^{-1}$) for the most densely cross-linked **MM40**. Intermediate values of these parameters were observed for **MM20** and **MM30**. These findings are consistent with the previous results.

Comparing the dynamics in the two dimensional scales, we notice that, in the millimeter-samples, the bending time was generally longer than the recovery time, whereas in the micro-actuators, the time needed for the contraction did not show a clear trend with respect to the recovery one. The overall picture derived from the above data indicate that combination of materials, with different mechanical behaviors, can be a smart and easy strategy to obtain robotic arms.

In particular, according to the "scallop theorem",[17] the easiest structure able to perform asymmetric motion presents two hinges as depicted in Fig. 7a. It can swim if the two hinges change their shape and then go back to the original position by a different sequence of movements, breaking the symmetry of the whole movement cycle. This effect can be realized by the combination of different LCNs in a single micro-actuator, exploiting a two-step DLW process. So far, this technique has been described for the integration of a single LCN mixture with a commercial resist with high rigidity[8] but not for combining different photo-responsive materials.

To achieve this aim, we prepared a stripe composed of a splayed cantilever of **MM40** polymer (Fig. 7b) linked to an analogous splayed cantilever prepared from **MM10** (Fig. 7c). After the fabrication of the first stripe, the LC cell was opened and developed in toluene, leading the LCN blocks on the homeotropic PI coated glass. This substrate was used to prepare a second splayed cell that was infiltrated with the second mixture. Then, the second writing step was performed. A correct alignment of the mixtures during the whole process is guaranteed only if the polymeric structures were anchored on the homeotropic coated glass. On the other hand, homogenous planar glasses suffer damage of the rubbed layer probably during the development process. By the use of a micromanipulator setup, it was possible to detach the whole structure and to observe its movement under the irradiation with the green laser.

Fig. 7d and e highlights the asymmetry in the movement of the composed splayed cantilever, due to the different rigidity of the stripe sides. In this geometry, the tip position also influenced the movement. Detailed observations of the movement dynamics were carried out with a fast camera (Fig. 7f). As expected, the maximum bending is reached by the two sides of the strip in two different times: the **MM10** stripe moved faster than the **MM40** arm (9 and 16 ms, respectively) creating a non-symmetric movement of the structure. The release to the equilibrium position, for each arm, occurred with an analogous relaxation time as already found resulting in a non-reciprocal motion when the whole sequence is considered.

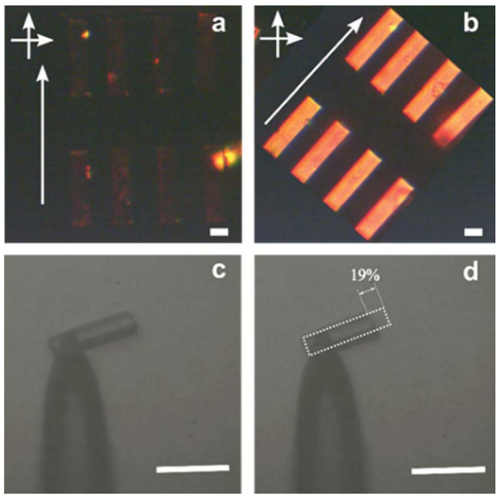

Fig. 6 DLW blocks fabricated with **MM10** mixture and their contraction under irradiation. (a) and (b) POM images of different blocks, respectively, parallel and at 45° in respect to the polarizer direction. The scale bar is 20 μm. (c) and (d) Optical image of a block suspended on a fiber, respectively, in the equilibrium position (no green laser excitation) and under a green laser light exposition. The scale bar is 80 μm.

Table 1 Contraction, expansion times (t_{cont} and t_{exp}), average contraction and expansion speeds (v_{cont} and v_{exp}) and maximum light-induced contraction of LCN blocks prepared by DLW

	t_{cont} (ms)	v_{cont} (μm ms^{-1})	t_{exp} (ms)	v_{exp} (μm ms^{-1})	Max contraction
MM10	12	1.26	16	0.95	19%
MM20	20	0.64	20	0.64	16%
MM30	20	0.68	16	0.85	17%
MM40	16	0.5	16	0.5	10%

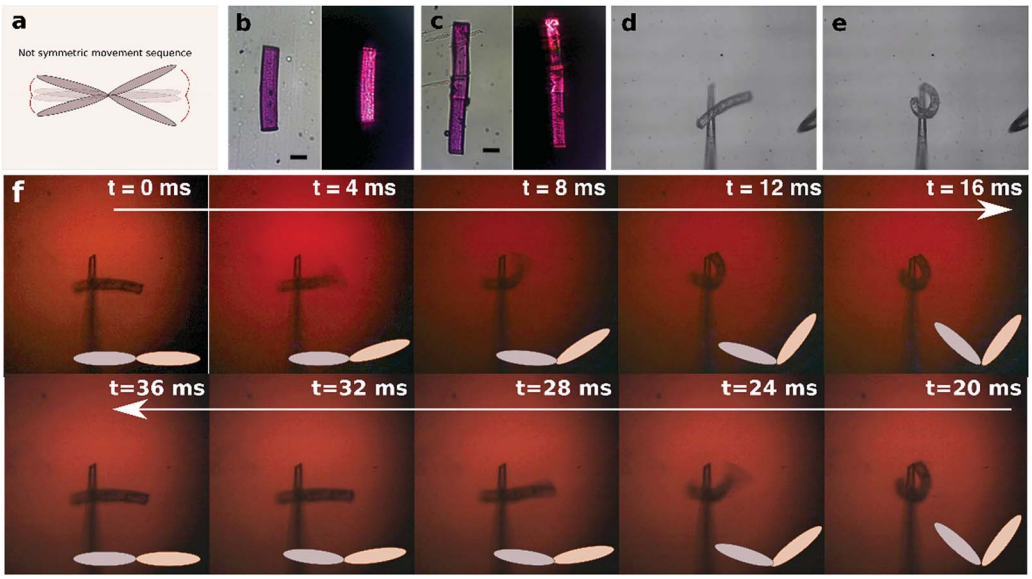

Fig. 7 Fabrication and activation of a stripe with arms prepared by two different LCN mixtures (**MM10** and **MM40**). (a) Scheme of a non-symmetric movement sequence (ref. 17); (b) a cantilever prepared by mixture **MM40** in a splayed cell after development and its POM image demonstrating the LC alignment; (c) a double materials stripe obtained after a second DLW process and development retaining the desired LC alignment as shown in POM images. The scale bar is 20 μm; (d) optical image of a stripe suspended on a fibre, in the equilibrium position (no green laser light excitation) and (e) under a green laser light irradiation; (f) sequence of fast camera video frames for the stripe bending and relaxation.

Experimental section

General procedures and materials

Molecules **1** and **2** were purchased by Synthon Chemical, Irgacure 369 was purchased from Sigma Aldrich and **3** was prepared as previously described.[15] ATR (attenuated total reflectance) spectra were obtained on an Infrared imaging microscope IN10 spectrophotometer (Thermo Fisher Scientific). Differential scanning calorimetry (DSC) was carried out using a Mettler-Toledo DSC 821 apparatus. Samples of about 5 mg were used and dry nitrogen was used as purge gas. Polarized optical microscopy (POM) was performed using the inverted microscope Zeiss, Axio Observer A1 with cross polarizers. Dynamic-mechanical analysis (DMA) was carried out by using a Rheometric DMTA V analyzer, employing rectangular tension geometry. The strain was sufficiently small to be within the linear viscoelastic range (0.1%) at the frequency of 1 Hz. An initial static force of 20 g was applied and a scanning rate of 4 °C min^{-1} was chosen in the range between −50 °C and temperature at which the film broke. Specimens were cut into bars with size of 20 × 5 × 0.02 mm^3. Change of mechanical modulus was monitored using a Rheometric DMTA V analyzer, employing rectangular tension geometry, at room temperature during the irradiation with a green LED lamp (Thorlabs M505L3-C1, 505 nm, 7 mW cm^{-2}), point are collected every 5 seconds due to instrumental specifications. An infrared thermometer IRT20 (Measupro) was used to control the real temperature on the specimens during the irradiation test.

LCN film preparation

Polymerization cells were prepared by means of differently coated glasses (coating was chosen in order to reach the desired liquid crystalline alignment of the mixture) with a 20 μm spacer. Homogeneous cells were prepared by the use of two PVA coated glasses after rubbing with a velvet cloth, while splayed cells were prepared by a rubbed PVA coated glass on the bottom and a PI1211 coated glass on the top. The mixtures were melted on a hot plate at 75 °C and then infiltrated by capillarity in the cells. Afterwards, the cells were cooled down to 45 °C and irradiated for 10 minutes with an UV LED lamp (Thorlabs M385L2-C4, 385 nm, I: 4 mW cm^{-2}, absorption and emission spectra of the dye and the lamp, respectively, are reported in Fig. S5†).

Finally, they were heated to 65 °C and irradiated for further 10 minutes. After polymerization, cells were opened and the films removed and tested without further purification.

Direct Laser Writing (DLW) fabrication

Two-photon absorption polymerization was induced by a focused laser beam from a 780 nm femtosecond laser in a commercial DLW workstation (Photonic Professional, Nanoscribe GmbH). The laser delivers 130 fs pulses with a 100 MHz repetition rate. Beam power was measured before the microscope objective. The laser beam was circularly polarized and focused with a 10X, 0.3 NA (Zeiss, EC Plan-Neofluar). The sample position was controlled by a 3D piezo translation stage. The structures were written on the bottom inner surface of a glass cell (laser power: 30 mW, scan speed: 90 μm s^{-1}) and after laser writing, the cell was opened and developed in a bath of toluene. After 2 minutes, the glass was dried with clean air.

100 × 20 × 10 μm^3 LCN blocks were fabricated using cells prepared by two uniaxially rubbed polyimide PI130 (Nissan Chemical Industries) coated glasses and filled with monomer mixtures as described in the previous section.

For the double cantilever, we used a splayed cell and the structures were written on PI1211 coated glass. First, the cell was filled with **MM40** and the blocks (100 × 20 × 8 μm^3) were written and developed in toluene. Afterward, another splayed LC cell was mounted by adding a PVA rubbed glasses on the top of the glass with such blocks. Cell was filled with **MM10** and the writing process was repeated. The second block was written overlapping the first one to ensure the adhesion/attachment of the different polymeric materials.

Light-induced movement

Macroscopic cantilever specimens (10 × 3 × 0.02 mm^3) were prepared by cutting splayed films and tested by illumination with a DPSS 532 nm laser from the top. Only a part of the actuator was illuminated due to the laser spot (5 mm of diameter) and the movement was recorded with a camera (50 fps). Light intensity was varied using a neutral density wheel-filter.

To test microstructures, actuators were detached with a home-made micromanipulator setup with the help of two glass tips after cells heating at 100 °C on a hot-stage (Linkam THM 600). The pre-heating step resulted needful to decrease their stiffness to the cell. Once obtained such freestanding blocks, light-induced deformations were observed during irradiation with a chopped (10 Hz and 50 Hz) DPSS 532 nm laser through a 10X, 0.25 NA (Plan Achromat, Olympus) objective placed above the sample (power density 100 mW mm^{-2}). The movement movies are recorded by an ultra-high speed fast camera (Photron FASTCAM SA4) with a recording frame rate of 250 fps frequency that allowed acceding to the contraction/elongation dynamics during the modulation period.

Conclusions

Different elastic moduli and response times emerged from the different polymeric architectures both at the macro- and micro-scales. Testing the materials with different light sources allowed to discriminate among the effects that contribute to the light induced movement. Deformations resulting from the *trans–cis* isomerization of the azobenzene in response to low power irradiation increase as the cross-linker percentage increases, while for the thermal effect by high power irradiation the trend is opposite with a defined dependence of the actuation times on the cross-linking density of the networks.

Integration of different LCN stripes by DLW into a monolithic actuator allowed to obtain a robotic arm able to perform asymmetric movements under a flat illumination. Such actuator deformed with different velocities at the two ends resulting in non-reciprocal movements of interest in complex robotic structures such as microswimmers. Even though other techniques to control the mechanical responses of LCN structures can be adopted to obtain modulated responses (*e.g.* use of structured light field, engineering of the geometrical shape of the devices), the control of light response by adjusting the cross-linker content in the mixture results to be a simple and unique method to enable further miniaturization of robotic devices. In fact, such behavior depends only on the material properties and is not connected to the spatial/temporal resolution of the applied stimuli. We end up with a versatile technique to create miniaturized devices controllable down to the nanometer scale.

Acknowledgements

The research leading to these results has received funding from the European Research Council under the European Union's Seventh Framework Programme (FP7/2007–2013)/ERC grant agreement n° [291349] on photonic micro robotics.

Notes and references

1 C. Ohm, M. Brehmer and R. M. Zentel, *Adv. Mater.*, 2010, **22**, 3366.
2 A. M. Flatae, M. Burresi, H. Zeng, S. Nocentini, S. Wiegele, C. Parmeggiani, H. Kalt and D. S. Wiersma, *Light: Sci. Appl.*, 2015, **4**, e282.
3 L. de Haan, A. P. H. J. Schenning and D. J. Broer, *Polymer*, 2014, **55**, 5885.
4 T. Ikeda, J. I. Mamiya and Y. Yu, *Angew. Chem., Int. Ed.*, 2007, **46**, 506.
5 M. Yamada, M. Kondo, J.-i. Mamiya, Y. Yu, M. Kinoshita, C. J. Barrett and T. Ikeda, *Angew. Chem.*, 2008, **47**, 4986.
6 C. Futao, Z. Yuanyuan, Y. Chu-Chun and Y. Yanlei, *Soft Matter*, 2010, **6**, 3447.
7 C. L. van Oosten, C. W. M. Bastiaansen and D. J. Broer, *Nat. Mater.*, 2009, **8**, 677.
8 H. Zeng, P. Wasylczyk, C. Parmeggiani, D. Martella, M. Burresi and D. S. Wiersma, *Adv. Mater.*, 2015, **27**, 3883.
9 S. Palagi, A. G. Mark, S. Y. Reigh, K. Melde, T. Qiu, H. Zeng, C. Parmeggiani, D. Martella, A. Sanchez-Castillo, N. Kapernaum, F. Giesselmann, D. S. Wiersma, E. Lauga and P. Fischer, *Nat. Mater.*, 2016, **15**, 647.
10 H. Finkelmann, H.-J. Kock and G. Rehage, *Makromol. Chem., Rapid Commun.*, 1981, **2**, 317.

11 D. Liu and D. J. Broer, *Langmuir*, 2014, **30**, 13499.
12 T. J. White and D. J. Broer, *Nat. Mater.*, 2015, **14**, 1087.
13 A. L. Elias, K. D. Harris, C. W. M. Bastiaansen, D. J. Broer and M. J. Brett, *J. Mater. Chem.*, 2006, **16**, 2903.
14 A. Buguin, M.-H. Li, P. Silberzan, B. Ladoux and P. Keller, *J. Am. Chem. Soc.*, 2006, **128**, 1088.
15 H. Zeng, D. Martella, P. Wasylczyk, G. Cerretti, J.-C. Gomez-Lavocat, C.-H. Ho, C. Parmeggiani and D. S. Wiersma, *Adv. Mater.*, 2014, **26**, 2319.
16 H. Zeng, P. Wasylczyk, G. Cerretti, D. Martella, C. Parmeggiani and D. S. Wiersma, *Appl. Phys. Lett.*, 2015, **106**, 111902.
17 E. M. Purcell, *Am. J. Phys.*, 1977, **45**, 3.
18 S. Nocentini, D. Martella, C. Parmeggiani and D. S. Wiersma, *Materials*, 2016, **9**, 525.
19 H. Shahsavan, S. M. Salili, A. Jákli and B. Zhao, *Adv. Mater.*, 2015, **27**, 6828.
20 R. A. M. Hikmet and D. J. Broer, *Polymer*, 1991, **32**, 1627.
21 H. M. D. Bandara and S. C. Burdette, *Chem. Soc. Rev.*, 2012, **41**, 1809.
22 J. Garcia-Amóros, M. C. R. Castro, P. Coelho, M. M. M. Raposo and D. Velasco, *Chem. Commun.*, 2016, **52**, 5132.
23 L. B. Braun, T. G. Linder, T. Hessberger and R. Zentel, *Polymers*, 2016, **8**, 435.
24 Y. Yu, M. Nakano, A. Shishido, T. Shiono and T. Ikeda, *Chem. Mater.*, 2004, **16**, 1637.
25 C. L. van Oosten, K. D. Harris, C. W. M. Bastiaansen and D. J. Broer, *Eur. Phys. J. E*, 2007, **23**, 329.
26 K. M. Lee and T. J. White, *Macromolecules*, 2012, **45**, 7163.
27 G. N. Mol, K. D. Harris, C. W. M. Bastiaansen and D. J. Broer, *Adv. Funct. Mater.*, 2005, **15**, 1155.